XL CILAMCE
IBERO-LATIN AMERICAN CONGRESS ON COMPUTATIONAL METHODS IN ENGINEERING
NOVEMBER 11-14, 2019
Praiamar Natal Hotel & Convention
Natal, RN-BRAZIL

NONLINEAR ELASTIC TRANSIENT ANALYSIS OF STEEL FRAMES WITH SEMI-RIGID CONNECTIONS

Harley F. Viana
Marília C. S. P. Salles
Renata G. L. Silva
harley-viana@hotmail.com
mariliapenido@yahoo.com.br
rglanna.silva@gmail.com
Federal Center for Technological Education of Minas Gerais
7675 Amazonas Avenue, 30510-000, Minas Gerais, Brazil
Armando C. C. Lavall
lavall@dees.ufmg.br
Federal University of Minas Gerais
6627 Pres. Antônio Carlos Avenue, 31270-901, Minas Gerais, Brazil
Rodrigo S. Costa
rodrigo.sernizon@ufba.br
Federal University of Bahia
Augusto Viana Street, 40110-909, Bahia, Brazil

Abstract. Steel structures are reputed to have high slender ratio and excellent ductility. Due to these features, the second-order effects and the influence of connection flexibility can play an important role on the behavior of such structures since they can increase the risk of instability. Additionally, it has been observed that only the linear static analysis may not describe the real behavior of a structure submitted to various external requests, especially in the case of atypical situations, such as earthquakes and strong wind gusts. Thus, the aim of this research is to evaluate the repercussion of the geometrical nonlinearity and connection flexibility on the transient elastic response of plane steel frames. To this end, it is employed a geometrically exact nonlinear formulation, based on Euler-Bernoulli model, that considers the updated Lagrangian formulation and the corotational approach for the consistent deduction of the element's tangent stiffness matrix. The theory predicts that nodes will suffer large displacements and rotations, and the elements of the structure, large stretches and curvatures. The semi-rigid connection is modelled by a rotational spring element whose behavior is obtained on the basis of a bilinear moment-rotation diagram that follows the kinematic hardening rule. In order to solve the nonlinear transient equations, it is adopted the Newmark's implicit time integration method combined with the Newton-Raphson technique. The results of the performed analyzes showed a good agreement with the numerical solutions available in the literature, demonstrating the efficiency of the proposed method in obtaining the geometrically nonlinear dynamic response of steel structures with semi-rigid connections.

Keywords: Geometrical nonlinearity, Dynamic analysis, Semi-rigid connections.

1 Introduction

In most designs of steel frames the beam-to-column connections are assumed to behave either as perfectly pinned or as fully rigid. Nonetheless, this assumption may conduct to an incorrect estimation of the frame behavior since the connections behave between those extremes. In reality, the beam-to-column connections exhibit a nonlinear moment-rotation relationship, which influences the overall stability of the structure as well as the distribution of the forces on its elements [1]. Besides, in the case of structural systems subjected to dynamic loadings, it is essential to consider the cyclic behavior of the connections. Considering this fact, a large number of interesting studies have been conducted to investigate the hysteretic response of beam-to-column connections [2][3][4][5][6].

Silva et al. [3] presented a numerical methodology to obtain the nonlinear transient response of planar structural systems with semi-rigid joints. The semi-rigid element stiffness matrix was deduced considering both the second-order effects and the connection flexibility. In order to predict the joint behavior under cyclic excitation an independent hardening model was employed.

Nguyen and Kim [4] proposed a numerical procedure for nonlinear dynamic elastic analysis of semi-rigid space steel frames. To simulate the joint behavior the authors used an independent zero-length element with six translational and rotational springs, which was used to connect two different nodes with identical coordinates.

Da Silva et al. [7] developed a modeling strategy to represent the dynamic behavior of semi-rigid connections by using the ANSYS finite element software. A rotational spring nonlinear element was used to consider the effect of connection flexibility. The authors emphasized that the nonlinear and hysteretic effects can significantly change the dynamic response amplitude of the structure. Therefore, these features are very important for an economic design of steel frames.

Lui and Lopes [8] presented results of a numerical study of semi-rigid frames under dynamic excitations. The connection's flexibility, in contrast to the studies cited above, were modelled by rotational springs with bilinear moment-rotation relationships, which follows the kinematic hardening rule. Similarly to the study of Nguyen and Kim [4], Lui and Lopes[8] employed stability functions in the formulation of the frame stiffness matrix to take into account the geometrical nonlinearities in terms of P-Δ and P-δ effects.

Recently, Koriga et al. [9] investigated the dynamic response of rigid and semi-rigid connections of steel structures under dynamic loads. The novelty of the nonlinear model consists in adopting only one bar element that accounts for the semi-rigid connection. Thus, there is no need to discretize the structural member in the program where nonlinearity is considered by a flexibility factor in the stiffness matrix.

This paper presents a numerical study of the geometrically nonlinear elastic dynamic behavior of steel frame structures with semi-rigid connections. The numerical procedure proposed in da Silva et al. [10] is extended for dynamic analysis of plane steel frames. Nevertheless, the shear deformation effect and the material nonlinearity are not considered in this study. The adopted formulation considers the updated Lagrangian formulation and the corotational approach for the consistent deduction of the element's tangent stiffness matrix. By using the concept of the corotational method the proposed theory allows that nodes undergo large displacements and rotations and the elements of the structure, large elongations and curvatures. In order to predict the nonlinear connection response it is applied zero-length spring element whose behaviors is obtained on the basis of moment-rotation curves. The advantage of this strategy is that no modification of the beam-column stiffness matrix is required to consider the semi-rigid connections. The solution of the transient equations are accomplished by combining the Newton-Raphson algorithm with the Newmark's implicit time integration method.

The described solution strategy was implemented in the PPLANLEP program, which is written in Fortran 90 language, and is capable to perform static and dynamic advanced analysis of frame steel structures. This program was developed by Lavall [11], adapted by Silva [12], who included the influence of semi-rigid connections and the shear deformations along the bars, and then modified by Viana [13], who included the dynamic analysis in the structure of the program.

The numerical responses obtained by the PPLANLEP program are compared with the numerical solutions available in the literature in order to demonstrate the efficiency and accuracy of the proposed method in obtaining the geometrically nonlinear dynamic response of steel structures with semi-rigid connections.

2 Nonlinear finite element

The formulation presented in da Silva et al. [10] is adopted in this study. In this formulation, the updated Lagrangian approach is employed. Thus, in the solution process, the aspects of the configuration to be obtained at the current instant **t+Δt** are related to the quantities determined at the previous instant **t**. The frame element in its reference and deformed configurations is illustrated in Fig. 1. The displacements that each joint suffers are denoted by **u**, displacement along **x** axis, **v**, displacement along **y** axis, and, **θ,** the rotation. Between the **a** and **b** extremities of the element it is defined a chord with length equal to $\mathbf{l_r}$. Then, a local reference coordinate system ($\mathbf{x_r}$,$\mathbf{y_r}$) with origin at the center of this chord is introduced. The angle between the global reference axis **x** and the chord is denoted by $\boldsymbol{\varphi_r}$. At current configuration, the chord between element nodes has length $\mathbf{l_c}$. A corotational coordinate system ($\mathbf{x_c}$,$\mathbf{y_c}$) is defined on this chord with origin at its center. The angle between the global reference axis **x** and the chord is now $\boldsymbol{\varphi_c}$, while the angle between the chord and the tangent to the element axis is α.

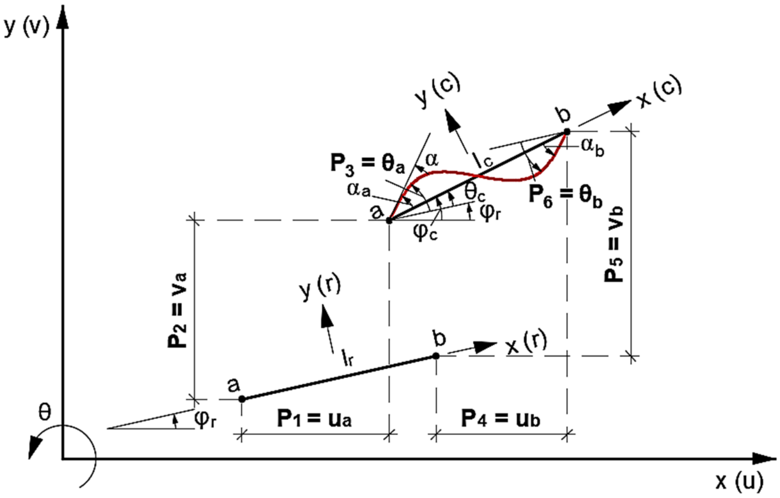

Figure 1. Element of a plane frame in its reference and deformed configurations

The freedom degrees to be adopted are those referent to the corotational system. The degrees of freedom can be collected in a vector q_ω, where ω = 1, 2, 3. The relations between natural and Cartesian degrees of freedom are listed below:

$$\begin{cases} q_1 = l_c - l_r \\ q_2 = \alpha_a = \theta_a - \theta_c = P_3 - \varphi_c + \varphi_r \\ q_3 = \alpha_b = \theta_b - \theta_c = P_6 - \varphi_c + \varphi_r \end{cases} . \quad (1)$$

where:

$$\begin{cases} l_c = \left[(x_b - x_a + P_4 - P_1)^2 + (y_b - y_a + P_5 - P_2)^2\right]^{1/2} \\ l_r = \left[(x_b - x_a)^2 + (y_b - y_a)^2\right]^{1/2} \\ \sin\varphi_c = \dfrac{y_b - y_a + P_5 - P_2}{l_c}; \quad \cos\varphi_c = \dfrac{x_b - x_a + P_4 - P_1}{l_c} \\ \varphi_c = \arctan\left(\dfrac{y_b - y_a + P_5 - P_2}{x_b - x_a + P_4 - P_1}\right); \quad \varphi_r = \arccos\left(\dfrac{x_b - x_a}{l_r}\right) \end{cases} . \quad (2)$$

In Eq. (2), x_a, x_b, y_a and y_b are the element nodal coordinates at reference configuration.

The Euler-Bernoulli hypothesis is employed in this study. Therefore, the displacement field of an arbitrary point in the beam element is defined if the axial displacement $u_c(x,y)$ and lateral displacement $v_c(x,y)$ of neutral axis are known, as well as the rotation of the transverse section α, according to Fig. 2.

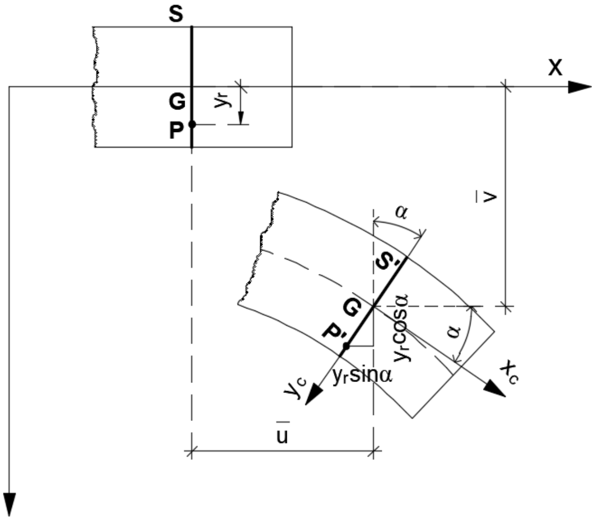

Figure 2. Displacement field considering the Euler-Bernoulli hypothesis

Suppose that the rotation angle is small, thus the displacements of the point **P** of section **S**, consistent with the Euler Bernoulli theory, can be written in the following form:

$$u_c(x,y) = \bar{u}_c(x) - y_r \alpha . \tag{3}$$

$$v_c(x,y) = \bar{v}_c(x) - y_r \frac{\alpha^2}{2} . \tag{4}$$

where, $\bar{u}_c$ and $\bar{v}_c$ are the displacements of the bar axis in the corotational system.

The rotation α of the cross sections results from the displacements $\bar{u}_c$ and $\bar{v}_c$ of the points on the bar's axis:

$$\alpha = \frac{\bar{v}'_c}{1 + \bar{u}'_c} . \tag{5}$$

Although the hypothesis of small rotations of the axis of the element in relation to its chord is adopted, the formulation does not lose its generality due to the use of the corotational system. It allows the occurrence of large displacements and curvatures as long as the elements used are sufficiently short.

Disregarding the higher order terms, the analytical expressions of the deformation field consistent with the adopted structural theory can be given by:

$$\varepsilon_x = \frac{du}{dx} = \frac{d\bar{u}}{dx} - y_r \frac{d\alpha}{dx} = \bar{\varepsilon}_x - y_r \alpha' . \tag{6}$$

The elongation of a fiber from the bar axis is calculated by

$$\bar{\lambda} = \left(1 + \bar{u}'_c\right) \sec \alpha . \tag{7}$$

The longitudinal deformation of the fiber from the bar axis can be obtained by

$$\bar{\varepsilon} = \bar{\lambda} - 1 . \tag{8}$$

Thus, the analytical expression of the deformation field becomes:

$$\varepsilon_x = \left(1 + \bar{u}'_c\right) \sec \alpha - 1 - y_r \alpha' . \tag{9}$$

Adopting second-order approximations for the trigonometric function, Eq. (9) can be written as:

$$\varepsilon_x = \left(1+\overline{u}_c'\right)\left(1+\frac{\alpha^2}{2}\right)-1-y_r\alpha' . \tag{10}$$

A stiffness matrix is then built for the element, getting to the expression:

$$k_{ij} = q_{\omega,i}\, D^f_{\omega,\beta}\, q_{\beta,j} + q_{\omega,i}\, H^f_{\omega,\beta}\, q_{\beta,j} + Q_\omega\, q_{\omega,ij} . \tag{11}$$

where

$$Q_\omega = \int_{V_r} \sigma_x\, \varepsilon_{x,\omega} dV_r . \tag{12}$$

$$D^f_{\omega,\beta} = \int_{V_r} \varepsilon_{x,\omega}\, D_f\, \varepsilon_{x,\omega}\, dV_r . \tag{13}$$

$$H^f_{\omega,\beta} = \int_{V_r} \sigma_x\, \varepsilon_{x,\omega\beta}\, dV_r . \tag{14}$$

where comma indicates partial differentiation. Note that Greek indices range from 1 to 3, while Latin indices range from 1 to 6.

In Eq. (11), the first part represents the constitutive portion, the second one and third one constitute the geometrical portion formed by the effects P-δ and P-Δ, respectively. As the material nonlinearity including gradual yielding of a steel beam–column member under axial force and bending moments is beyond the scope of this study, the constitutive matrix remains elastic.

For more details of this formulation, refer to the work of da Silva et al. [10].

3 Semi-rigid connections

3.1 Modeling of connection moment-rotation behavior

The flexibility of the beam-to-column connections is given by a nonlinear moment-rotation curve. These curves can be obtained from experimental tests, numerical simulation or theoretical models [3]. Fig. 3 shows different curve-adjustment techniques used in numerical analysis to idealize the moment-rotation relationship. The advantage of using these models is that they can prevent the occurrence of negative connection stiffness, which is not desirable for numerical computation [9]. Besides, they require only a small number of parameters as input for the analysis, making the procedure of computing the connection stiffness simpler and with less computational effort.

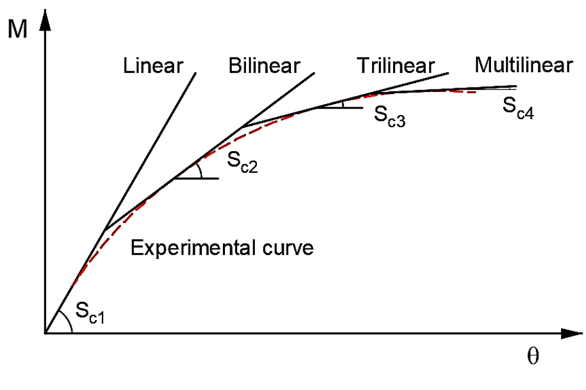

Figure 3. Mathematical models for moment-rotation relationship

The linear model has the advantage of simplifying the implementation since it uses the initial stiffness to represent all bonding behavior. Nonetheless, it becomes less accurate as the request increases, overestimating connection capability. Furthermore, the linear model neglects the energy dissipation at connections.

A significant improvement is obtained through the bilinear model, although it is not able to consider continuous changes in stiffness along the curve. By contrast, the trilinear and multilinear models can describe more precisely the moment-rotation relationship. Nevertheless, a higher degree of accuracy can be obtained by using nonlinear moment-rotation curves.

A popular model used for semi-rigid connections is the polynomial function proposed by Frye and Morris [14]. The model consists in approximating the experimental curve through a polynomial function that has the following form:

$$\theta_r = C_1(kM) + C_2(kM)^3 + C_3(kM)^5. \tag{15}$$

where, C_i is the curve-fitting constants and k is the standardization factor, which depends on the type and geometrical characteristics of the particular connection considered.

The disadvantage of this model is that the first derivative of this function may be discontinuous and or possibly negative for certain connection types [15]. Furthermore, after a specific loading limit, the model begins to show large discrepancies from the experimental curve.

Lui and Chen [16] proposed an exponential function to curve-fit the experimental moment-rotation curve. The mathematical expression for the moment-rotation relationship is established by the following equation:

$$M = M_o + \sum_{j=1}^{n} C_j \left(1 - \exp\left(-\frac{|\theta_r|}{2j\alpha}\right)\right) + R_{kf}|\theta_r|. \tag{16}$$

in which, M_o is the initial moment; M and θ_r are the moment and rotational deformation of the connection, respectively; C_j is the curve-fitting coefficient; n is the number of terms considered; R_{kf} is the initial strain-hardening stiffness of the connection and α is the scaling factor.

The Kishi–Chen three-parameter power model is another commonly used model for representing the behavior of the connections. The generalized form of this model is given by

$$M = \frac{R_{ki}\theta_r}{\left[1 + \left(\frac{\theta_r}{\theta_o}\right)^n\right]^{\frac{1}{n}}}. \tag{17}$$

where, R_{ki} is the initial connection stiffness; θ_o is the reference plastic rotation; n is the shape parameter; M and θ_r are the moment and rotation of the connection, respectively.

In 1975, Richard and Abbott proposed a four-parameter model [17]. The moment-rotation form of this model is defined by

$$M = \frac{(R_{ki} - R_{kp})|\theta_r|}{\left[1 + \left|\frac{(R_{ki} - R_{kp})|\theta_r|}{M_o}\right|^n\right]^{\frac{1}{n}}} + R_{kp}|\theta_r|. \tag{18}$$

in which, M and θ_r are the moment and the rotation of the connection, n is the shape parameter, R_{ki} is the initial connection stiffness, R_{kp} is the strain-hardening stiffness and M_o is the reference moment.

3.2 Semi-rigid connection model

The cyclic connection moment-rotation relationship is assumed to be bilinear and follows the kinematic hardening rule as presented in Fig. 4. Only three parameters are required to use this model, the initial stiffness R_{ki}, the strain hardening stiffness R_{kp} and the bound slope moment M_{bound}. Initially the connection stiffness is R_{ki}. Then, when the moment envelope is reached the stiffness changes from R_{ki} to R_{kp}. Upon loading and reloading, the connection stiffness reverts to R_{ki}. Nonetheless, if the moment in the connection due to unloading and reloading equals or exceeds that defined by the moment envelope, the connections stiffness will be R_{kp}.

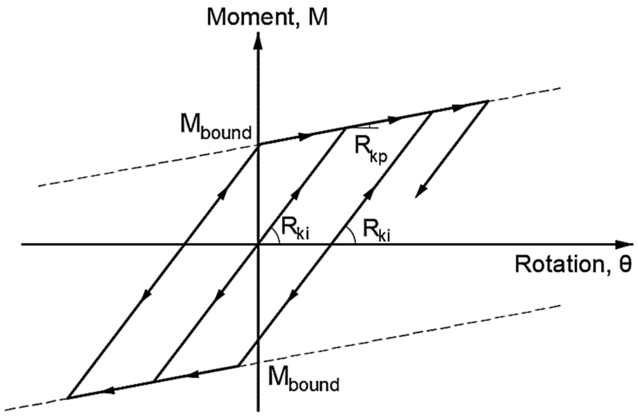

Figure 4. Kinematic hardening model

The values of R_{ki}, R_{kp} and M_{bound} are obtained by curve-fitting the available connection moment-rotation relationship.

4 Nonlinear dynamic analysis procedure

The Newmark's implicit time integration method combined with the Newton-Raphson iterative algorithm is adopted to solve the the differential equations of motion. Thus, the equilibrium at time **t + Δt** can be express as:

$$\mathbf{M}\ddot{\mathbf{U}}^{(t+\Delta t)} + \mathbf{C}\dot{\mathbf{U}}^{(t+\Delta t)} + \mathbf{K}\mathbf{U} = \mathbf{F}_{ext}^{(t+\Delta t)} - \mathbf{F}_{int}^{t} . \tag{19}$$

where **M**, **C**, **K** are the mass, damping and tangent stiffness matrices, respectively; $\ddot{\mathbf{U}}$, $\dot{\mathbf{U}}$ are vectors of nodal point accelerations and velocities, respectively; $\mathbf{U}$ is the vector of nodal point displacement increments; $\mathbf{F}_{ext}$ is the applied external load vector and $\mathbf{F}_{int}^{t}$ is the nodal point force vector equivalent to the element stresses.

In the present work, the mass matrix is lumped and the effects of rotary inertia are neglected. Since Rayleigh damping is adopted, the damping matrix is given by a linear combination of the mass and stiffness matrices:

$$\mathbf{C} = \mu_1 \mathbf{M} + \mu_2 \mathbf{K} . \tag{20}$$

where μ_1 and μ_2 are mass and stiffness proportional damping factors, rescpectively.

The Newmark's method consists in expressing the displacements and velocities according to finite difference approximations in the time domain, given by:

$$\mathbf{U}^{(t+\Delta t)} = \mathbf{U}^{t} + \Delta t\dot{\mathbf{U}}^{t} + \frac{\Delta t^2}{2}\left[(1-2\beta)\ddot{\mathbf{U}}^{t} + 2\beta\ddot{\mathbf{U}}^{(t+\Delta t)}\right]. \tag{21}$$

$$\dot{\mathbf{U}}^{(t+\Delta t)} = \dot{\mathbf{U}}^{t} + \Delta t\left[(1-\gamma)\,\ddot{\mathbf{U}}^{t} + \gamma\,\ddot{\mathbf{U}}^{(t+\Delta t)}\right]. \quad (22)$$

where γ and β are parameters that determine the stability and precision properties of the method.

5 Validation

The efficiency and accuracy of the proposed formulation are demonstrated by the following numerical examples. The responses obtained by the PPLANLEP program are compared with the numerical solutions available in the literature. In all analyzes, the parameters γ and β of the Newmark method are considered equal to 0.5 and 0.25, respectively. Rayleigh proportional damping is not considered during the analysis.

5.1 Clamped-clamped beam

A clamped-clamped beam under a concentrated load applied at the mid-span has been investigated by Chan and Chui [2], Cunha [18], Hsiao and Jang [19], and others (Fig. 5). The structure is subjected to a vertical impact load of 2.85 kN applied at the middle of the beam. The elements have a rectangular cross-sectional area of 0.8065 cm², inertia of 6.775 x 10^{-3} cm^4, longitudinal modulus of elasticity equal to 206.85 GPa and linear density equal to 2.7103 x 10^{-8} kNs²/cm^4. In the present study, the beam is divided into 10 elements, and the cross section was discretized into 20 slices. The stiffness of the semi-rigid connections is igual to S_c = EI/L. A constant time step of 10 μs and a tolerance of 10^{-4} for the displacements are adopted in this analysis.

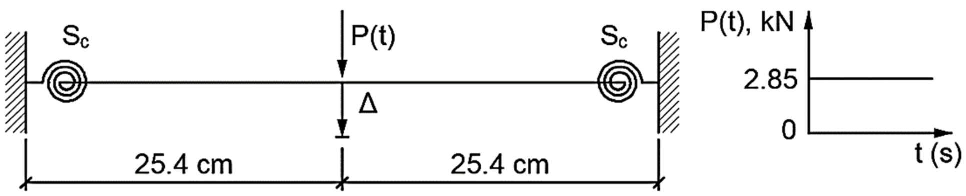

Figure 5. Clamped-clamped beam subjected to a dynamic impact load

The time-history of the mid-span displacement is given in Fig. 6. The results provided by the PPLANLEP program are in close agreement with the results reported by the mentioned authors.

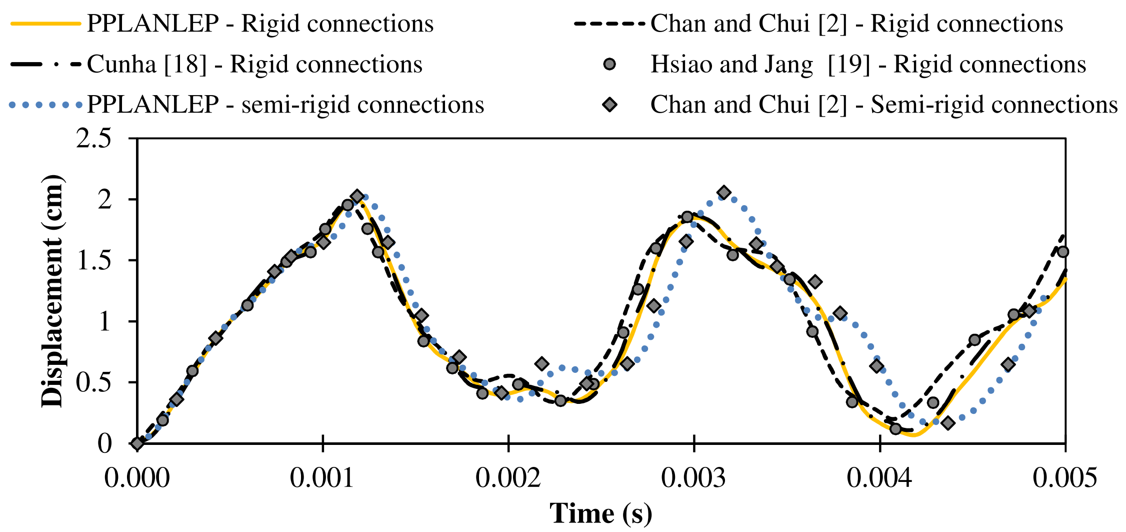

Figure 6. Dynamic response of clamped-clamped beam with different supports

The small differences between the obtained responses and those presented in the literature are related to the formulation adopted. In this research it was used the lumped mass matrix while the cited works employed a consistent mass matrix. As can be seen, the beam with flexibly connections has a longer period and a larger peak deflection.

5.2 Single-bay two-storey frame

The objective of this numerical example is to analyze the influence of gravitational forces and the semi-rigid connections on the geometrically nonlinear dynamic behavior of plane steel frames. The gravitational forces induce axial stresses on the columns and, consequently, cause a reduction in the stiffness of these members. In addition, additional moments are produced due to the P-Δ effect generated by these static loads.

Fig. 7 shows a single-bay two-storey frame with pinned supports. The beams of the structure are made of W14x48 profiles, while the columns, W12x96 profiles. A longitudinal modulus of elasticity E, equal to 205 GPa, is adopted for all structural members. Lumped masses of 3730 kg and 7460 kg are located at the ends and at the center of the beams, respectively. Two elements per beam member and only one element per column were used in the discretization of this structure. The cross sections were discretized into 50 slices, 20 for each flange and 10 for the web. The left columns are subjected to cyclic loads and the responses of displacements are compared with those presented by Chan and Chui [2]. Extended flush end plate connections, with an initial stiffness of 1,234,019.80 kN.cm/rad, are considered between the beams and the columns.

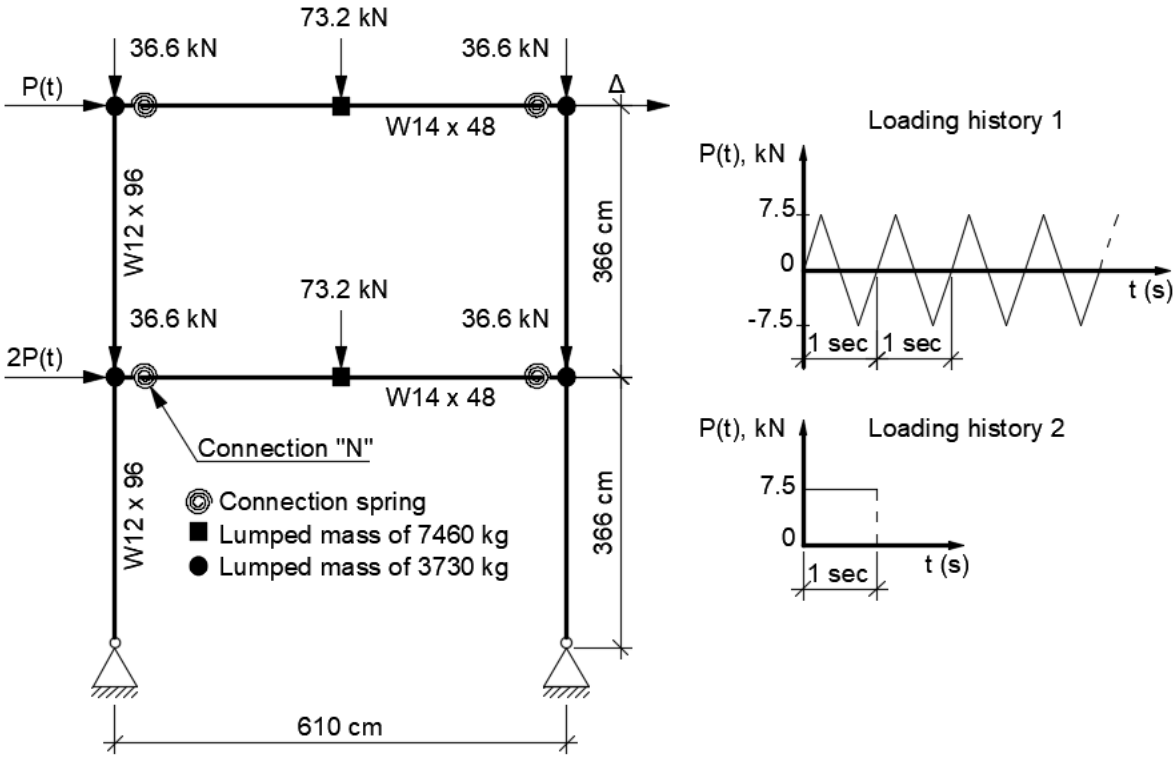

Figure 7. Single-bay two-storey frame: layout and loading

The moment-rotation relationships adopted in this example was obtained by curve-fitting the moment-rotation relationship represented by the Chen-Lui exponential model [16], as shown in Fig. 8.

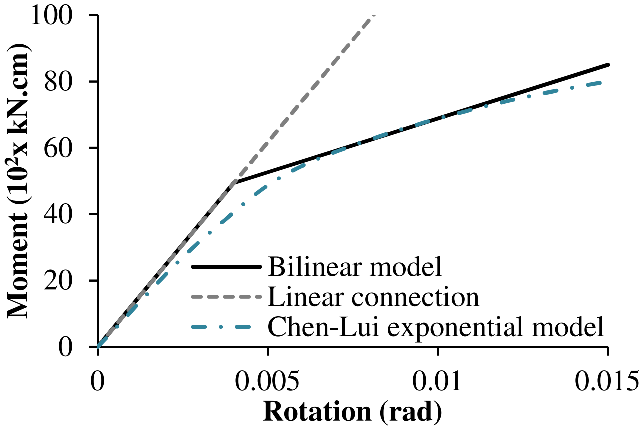

Figure 8. Moment-rotation curve of flush end plate connection

The parameters of the Chen–Lui exponential model for the flush end plate connection are listed in Table 1.

Table 1. Parameters of the Chen-Lui exponential model

M_o (kN.cm)	0
R_{ki} (kN.cm/rad)	1234019.80
α	0.31783x10^{-3}
C_1	-2828.90
C_2	57323.70
C_3	-343427.02
C_4	851200.97
C_5	-936334.62
C_6	383321.77
R_{kf} (kN.cm)	10893.38

Fig. 9 exhibits the time history of the horizontal displacement at the top right of the structure when it is considered cyclic loads (Loading history 1). In the transient state, the deflection reaches a maximum of around ± 7 cm. When the structure reaches the permanent regime, the deflection oscillates between ± 5 cm. It is important to highlight that gravitational loads were not included in this first analysis.

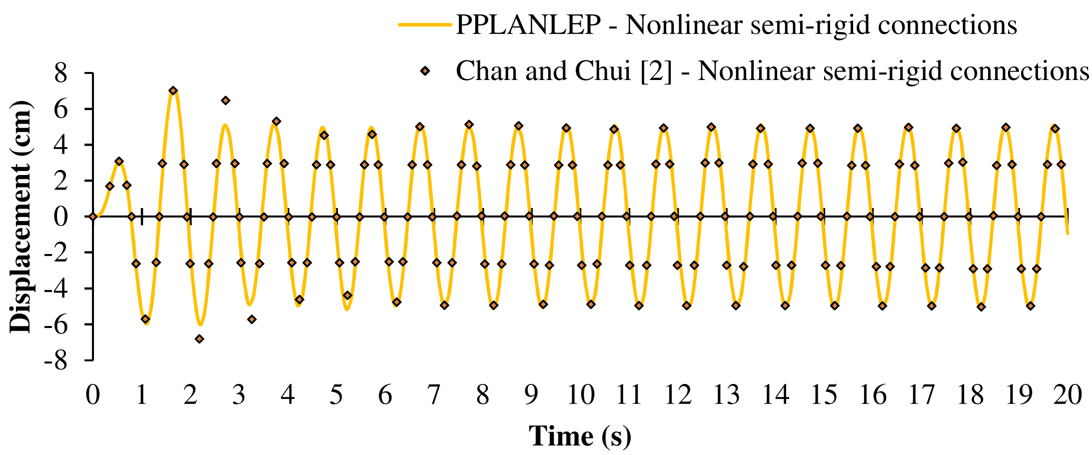

Figure 9. Time-displacement response of steel frame under cyclic load

Fig. 10 depicts the moment-rotation loops at connections during the incremental process. The amount of energy dissipated underlines the influence of the nonlinear moment-rotation behavior of the semi-rigid connections on the dynamic response of steel frames.

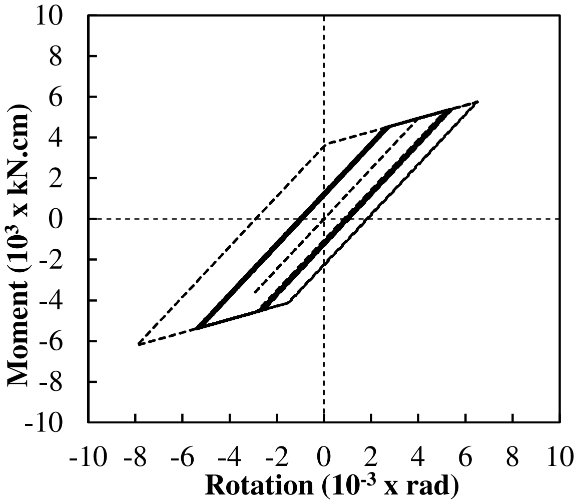

Figure 10. Moment-rotation hysteretic behavior at connection N

In order to more accurately predict the nonlinear dynamic behavior, it was considered gravitational loads statically applied to the ends and center of the beams with magnitudes of 36.6 kN and 73.2 kN, respectively. The structure was then analyzed considering a rectangular pulse of 7.5 kN acting during 1s (Loading history 2). For comparison purposes, analyzes were performed with the presence and absence of gravitational loads. A constant time increment of 0.005s and a tolerance of 10^{-4} for the displacements were used.

Fig. 11 and Fig. 12 show the time-displacement response of the same structure without and with the presence of the gravitational force, respectively, and considering various connection types. Again a good correlation is seen between the obtained results and those reported by Chan and Chui [2], especially for the cases with rigid and linear connections. The main reason of the small differences between the responses obtained for nonlinear connections are related to the adopted connection model. While Chan and Chui [2] used a nonlinear moment-rotation diagram and the independent hardening model to represent the moment-rotation behavior of connections under dynamic loading, the present study employed a bilinear moment-rotation relationship and the kinematic hardening rule.

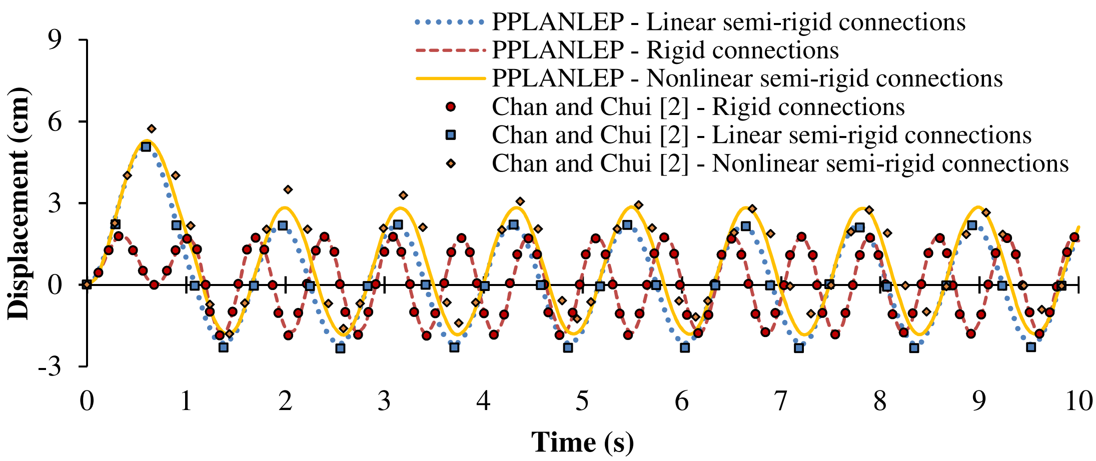

Figure 11. Dynamic response of single-bay two-storey frame with nonlinear connections under rectangular pulse – without gravity loads

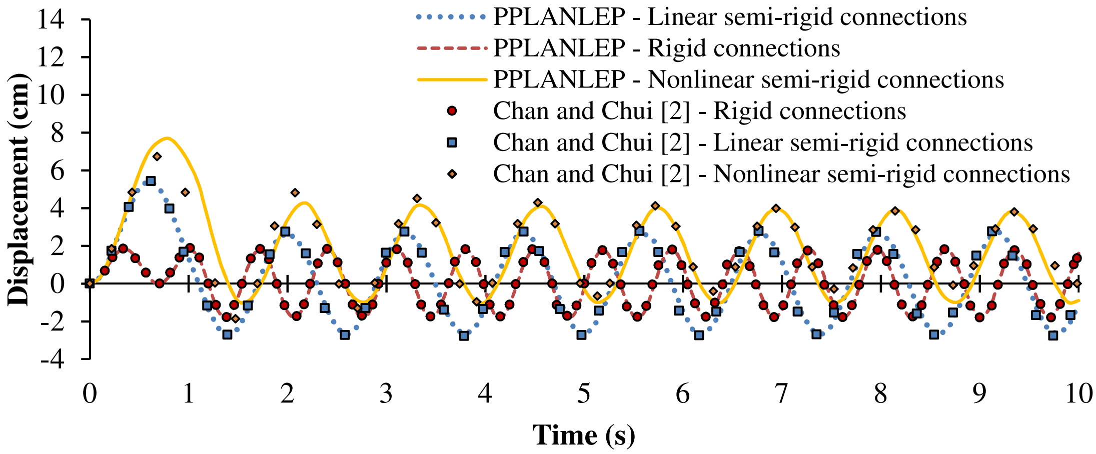

Figure 12. Dynamic response of single-bay two-storey frame with nonlinear connections under rectangular pulse – with gravity loads

It was noticed that the gravitational loads induced a small increase in the horizontal displacements, which is related to the reduction of the columns' stiffness by the P-Δ effect. When considering rigid connections this effect was smaller. Furthermore, it is seen that in the cases of flexibly jointed frames, the permanent rotations at the connections caused a shift of deflection responses. Therefore, the nonlinear connections plays an important role in the dynamic response of steel structures since the natural frequency changes when the joint stiffness varies.

6 Conclusion

This paper presented a numerical study of the geometrically nonlinear elastic dynamic behavior of semi-rigid steel frame structures. The formulation proposed in the work of da Silva et al. [10] was extended for dynamic analysis of plane steel frames, as described in Viana [13]. The present numerical procedure combines the updated Lagrangian description with the corotational technique for the consistent deduction of the tangent stiffness matrix of the element. The theory predicted that nodes will suffer large displacements and rotations, and the elements of the structure, large stretches and curvatures. The semi-rigid connection was modelled by a rotational spring element whose behavior was obtained on the basis of a bilinear moment-rotation diagram that follows the kinematic hardening rule. The Newmark time integration scheme combined with the Newton-Raphson iterative technique was adopted to solve the nonlinear incremental dynamic equilibrium equation in temporal domain. In order to reduce computational effort in the simulations, the lumped mass matrix was adopted.

It was found that the variation in the connection stiffness may decrease the natural frequency of the structure. Besides, the hysteretic behavior of the connections decreases the vibration amplitudes, which is beneficial for the safety of the structure. Based on the provided examples it was concluded that the nonlinear connections plays an important role in the dynamic response of planar steel structures.

Regarding the gravitational forces, it was observed that these static loads cause a reduction in the columns stiffness due to appearance of second-order effects. In the nonlinear connection case, this influence was larger if compared with the rigid and linear connection types.

In all analyzes, it was found good agreement with the results provided by previous studies, confirming the efficiency of the formulation and numerical solution strategy adopted. Thus, it is believed that the present formulation may represent a valuable engineering tool for the nonlinear transient analysis of planar steel structures undergoing large displacements and rotations.

Acknowledgements

The authors gratefully acknowledge the financial support of this research given by the Minas Gerais State Agency for Research and Development – FAPEMIG and the Federal Center for Technological Education of Minas Gerais - CEFET-MG.

References

[1] U. Dave and G. Savaliya, 2010. Analysis and Design of Semi-Rigid Steel Frames, in *Structures Congress*, pp. 3240–3251.

[2] S.-L. Chan and P.-T. Chui. *Non-linear static and cyclic analysis of steel frames with semi-rigid connections*. Elsevier, 2000.

[3] A. R. D. Silva, E. A. P. Batelo, R. A. M. Silveira, F. A. Neves, and P. B. Gonçalves. On the Nonlinear Transient Analysis of Planar Steel Frames with Semi-Rigid Connections: From Fundamentals to Algorithms and Numerical Studies. *Lat. Am. J. Solids Struct.*, vol. 15, no. 3, 2018.

[4] P.-C. Nguyen and S.-E. Kim. Nonlinear elastic dynamic analysis of space steel frames with semi-rigid connections. *J. Constr. Steel Res.*, vol. 84, pp. 72–81, 2013.

[5] A. Azizinamini and J. B. Radziminski. Static and cyclic performance of semirigid steel beam-to-column connections. *J. Struct. Eng.*, vol. 115, no. 12, pp. 2979–2999, 1989.

[6] M. N. Nader and A. Astaneh. Dynamic behavior of flexible, semirigid and rigid steel frames. *J. Constr. Steel Res.*, vol. 18, no. 3, pp. 179–192, 1991.

[7] J. G. S. Da Silva, L. R. O. De Lima, P. C. G. da S. Vellasco, S. De Andrade, and R. A. De Castro. Nonlinear dynamic analysis of steel portal frames with semi-rigid connections. *Eng. Struct.*, vol. 30, no. 9, pp. 2566–2579, 2008.

[8] E. M. Lui and A. Lopes. Dynamic analysis and response of semirigid frames. *Eng. Struct.*, vol. 19, no. 8, pp. 644–654, 1997.

[9] S. Koriga, A.-N. T. Ihaddoudene, and M. Saidani. Numerical model for the non-linear dynamic analysis of multi-storey structures with semi-rigid joints with specific reference to the Algerian code. *Structures*, vol. 19, pp. 184–192, 2019.

[10] R. G. L. da Silva, A. C. C. Lavall, R. S. Costa, and H. F. Viana. Formulation for second-order inelastic analysis of steel frames including shear deformation effect. *J. Constr. Steel Res.*, vol. 151, pp. 216–227, 2018.

[11] A. C. C. Lavall. Uma formulação teórica consistente para a análise não linear de pórticos planos pelo método dos elementos finitos considerando barras com imperfeições iniciais e tensões residuais na seção transversal. Tese de Doutorado, Universidade de São Paulo, São Carlos, 1996.

[12] R. G. L. Silva. Análise inelástica avançada de pórticos planos de aço considerando as influências do cisalhamento e de ligações semirrígidas. Tese de Doutorado, Universidade Federal de Minas Gerais, Belo Horizonte, 2010.

[13] H. F. Viana. Análise avançada dinâmica de pórticos planos de aço. Dissertação de Mestrado, Centro Federal de Educação Tecnológica de Minas Gerais, Belo Horizonte, 2019.

[14] M. J. Frye and G. A. Morris. Analysis of flexibly connected steel frames. *Can. J. Civ. Eng.*, vol. 2, no. 3, pp. 280–291, 1975.

[15] W.-F. Chen and N. Kishi. Semirigid steel beam-to-column connections: Data base and modeling. *J. Struct. Eng.*, vol. 115, no. 1, pp. 105–119, 1989.

[16] E. M. Lui and W.-F. Chen. Analysis and behaviour of flexibly-jointed frames. *Eng. Struct.*, vol. 8, no. 2, pp. 107–118, 1986.

[17] R. M. Richard and B. J. Abbott. Versatile elastic-plastic stress-strain formula. *J. Eng. Mech. Div.*, vol. 101, no. 4, pp. 511–515, 1975.

[18] J. P. F. B. da Cunha. Análise estática e dinâmica de pórticos planos com o uso da formulação corrotacional. Dissertação de Mestrado, Universidade Federal de Goiás, 2018.

[19] H. Kuo-Mo and J. Jing-Yuh. Nonlinear dynamic analysis of elastic frames. *Comput. Struct.*, vol. 33, no. 4, pp. 1057–1063, 1989.